

Mutants of Phosphorylase *a* Altered in Recognition by Protein Phosphatase-1<sup>†</sup>Cheryl Bartleson,<sup>\*,‡</sup> Alyssa C. Biorn,<sup>§</sup> and Donald J. Graves*Department of Biochemistry, Biophysics, and Molecular Biology, 1210 Molecular Biology Building, Iowa State University, Ames, Iowa 50011**Received October 31, 2002; Revised Manuscript Received January 22, 2003*

**ABSTRACT:** To develop our knowledge of specificity determinants for protein phosphatase-1, mutants of phosphorylase *b* have been converted to phosphorylase *a* and examined for their efficacy as substrates for protein phosphatase-1. Mutants focused on the N-terminal primary sequence surrounding the phosphoserine (R16A, R16E, and I13G) and at a site that interacts with the phosphoserine in phosphorylase *a*, (R69K and R69E). The success achieved studying protein kinase substrate specificity with peptide substrates has not extended to protein phosphatases. Protein phosphatases are believed to recognize higher order structure in substrates in addition to the primary sequence surrounding the phosphoserine or threonine. Peptide studies with protein phosphatase-1 have revealed a preference for basic residues N-terminal to the phosphoserine. Arginine 16 in phosphorylase *a* may be a positive determinant. In this work, protein phosphatase-1 preferred the positive charge on arginine 16. R16A exhibited a similar  $K_m$  but reduced  $V_{max}$ , and R16E had an increased  $K_m$  and a decreased  $V_{max}$  when compared to phosphorylase. I13G had a similar  $K_m$  but an increased  $V_{max}$ . The R69 mutants were also dephosphorylated preferentially over phosphorylase *a*. The  $K_m$  for R69K was unchanged but had a higher  $V_{max}$ . R69E exhibited the most changes, with a 4-fold increase in  $K_m$  and a 10-fold increase in  $V_{max}$ . These results suggest that proper presentation of the phosphoserine can greatly affect the rate of dephosphorylation.

Protein phosphatase-1 (PP-1)<sup>1</sup> is one of four major cytosolic serine/threonine phosphatases distinguished by substrate specificity and susceptibility to specific inhibitors (1). These phosphatases are designated phosphatases type-1, -2A, -2B, also known as calcineurin (CaN), and -2C. Little information is available on the specificity of PP-1. PP-1 is considered a broad specificity phosphatase. However, the best known physiological protein substrate for PP-1 is phosphorylase *a* (phos. *a*) (2). The wealth of knowledge of protein kinase specificity derived from peptide studies has not extended to the protein phosphatases. This could be due to the fact that phosphopeptides are not very good substrates for many phosphatases (3). Protein phosphatases seem to be less dependent on primary structure and more dependent on aspects of secondary structure for recognition of substrate.

Nevertheless, some information has been gained from phosphopeptide studies. The preference for basic residues N-terminal to the phosphoserine was found to be a general

determinant for PP-1 (3). An additional potential preference for a basic residue C-terminal to the phosphoserine might exist. Peptides derived from phos. *a* lacking the residue arginine 16 fail to function as PP-1 substrates (4). Modification of arginine 16 in peptide substrates by nitrosylation or amidation, and more recently through substitution with citrulline, indicates that a positive charge may be important for substrate recognition (5, 6). Analysis of the citrulline-substituted peptide substrates indicates that arginine 16 is important for enhanced turnover (6).

Attempts to study substrate specificity by mutagenesis of PP-1 have provided only limited information. The acidic groove of PP-1, proposed to bind the N-terminal basic residues found in many of its substrates, was extensively mutated. No major changes in the kinetic parameters for phos. *a* were observed with these mutants. The systematic mutagenesis involved changing only one amino acid at a time, however, which might have led to some compensation in the mutants by the surrounding acidic residues still available (7).

In this work, phosphorylase mutants were constructed to examine the specificity of the PP-1 catalytic subunit using a physiologically relevant protein substrate. The selected mutants changed the primary structure around the phosphorylatable site in the N-terminus of phosphorylase *b*, as well as the phosphoserine interaction site. The basic residue found at the P+2 position of phosphorylase (Arg16) was changed to Ala (R16A) and Glu (R16E). This arginine residue is a positive specificity determinant for phosphorylase kinase and is a potential positive determinant for PP-1 (8, 9). A hydrophobic residue in position P-1 was changed to glycine, I13G. This isoleucine is located in the 3<sub>10</sub> helical segment

<sup>†</sup> This work was supported by NIH Grant GM-09587 to D.J.G. and by an NSF Training Grant DIR9113595 graduate fellowship to C.B. and A.C.B. This is journal paper J-19381 of the Iowa Agriculture and Home Economics Experiment Station, Ames, Iowa, Project No. 3341, and supported by Hatch Act and State of Iowa funds.

\* To whom correspondence should be addressed. Phone: (615) 322-5268. Fax: (615) 322-5117. E-mail: cheryl.bartleson@vanderbilt.edu.

<sup>‡</sup> Current address: 444 Robinson Research Building, Department of Pharmacology, Vanderbilt University Medical Center, Nashville, TN 37232-6600.

<sup>§</sup> Current address: 409 Johnson Pavilion, 3610 Hamilton Walk, University of Pennsylvania, Philadelphia, PA 19104-6100. Phone: (215) 573-6640. Fax: (215) 349-5572.

<sup>1</sup> Abbreviations: PP-1, protein phosphatase-1; phos. *b*, phosphorylase *b*; phos. *a*, phosphorylase *a*; PP-2A, protein phosphatase-2A; AP, alkaline phosphatase; CaN, calcineurin.

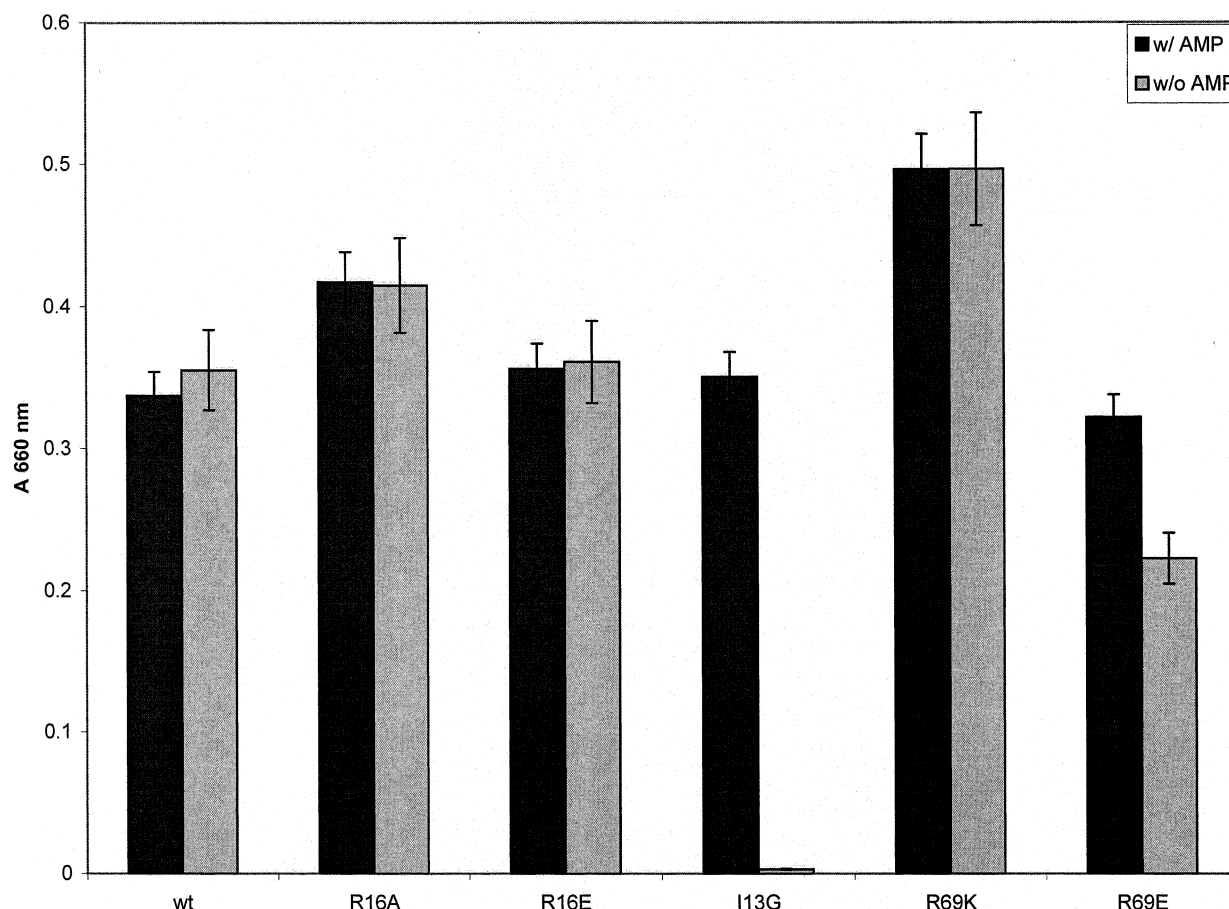


FIGURE 1: Phosphorylase *a* activities in the presence and absence of AMP. Phosphorylase *a* activity was assayed spectrophotometrically at A 660 nm using a concentration of 10  $\mu$ g/mL phosphorylase in the presence and absence of 1 mM AMP. Activities were assayed a minimum of three times in triplicate on at least three separate occasions with a minimum of three different protein preparations.

formed by the N-terminus in phos. *a*. Substituting glycine may disrupt the helical structure and make this region more conformationally flexible (10). The Arg 69 residue of phosphorylase participates in a salt bridge with the seryl phosphate of phos. *a*, which is thought to hold the phosphorylated N-terminus in place (11). Two mutants of this position were constructed, R69K and R69E. All mutant phos. *a*'s were compared to native phos. *a* with respect to substrate recognition by a variety of protein phosphatases, PP-1 in particular.

## EXPERIMENTAL PROCEDURES

**Materials.** All chemicals were commercially available from Boehringer Mannheim (Indianapolis, IN), Fisher (Pittsburgh, PA), or Sigma (St. Louis, MO). The truncated catalytic  $\gamma$  subunit of phosphorylase kinase,  $\gamma$ (1–300), was renatured as described (12). Recombinant PP-1 catalytic subunit was purchased from New England Biolabs (Beverly, MA). Alkaline phosphatase (AP) was available from Sigma. CaN was a generous gift of Dr. Bruce L. Martin. Protein phosphatase-2A (PP2A) was purchased from Upstate Biotechnology (Lake Placid, NY). [ $\gamma$ - $^{32}$ P]ATP was from ICN Biomedicals (Costa Mesa, CA).

**Preparation of Phosphorylase *b* and Mutant Phosphorylase *b*'s.** Phosphorylase *b* (phos. *b*) was purified as described (13). Mutants were constructed as described (9). Recombinant phos. *b*'s were expressed and purified as described (14,

15). Protein concentrations of phosphorylases were determined spectrophotometrically at 280 nm (16).

**Preparation of Phosphorylase *a* and Mutant Phosphorylase *a*'s.** Phos. *b* and mutant phos. *b*'s were converted to phos. *a* as described by Krebs and Fischer, with some modification (17). Truncated  $\gamma$ (1–300) was incubated with 1 mg/mL phosphorylase, 1 mM [ $\gamma$ - $^{32}$ P]ATP, 10 mM MgCl<sub>2</sub>, 5 mM dithiothreitol, 50 mM Pipes, and 50 mM Tris, pH 8.2. At a specified time, sample aliquots were removed from the reactions and spotted on ET-31 Whatman filter paper. Samples were washed and counted to determine the amount of radioactivity incorporated into phos. *a* (18).

Phos. *a* activity was measured in the presence and absence of AMP as described (19).  $^{32}$ P-phos. *a*'s were dialyzed into 50 mM imidazole, pH 7.2, 5 mM dithiothreitol and stored at 4 °C. AMP activation assays were performed monitoring phosphorylase activity spectrophotometrically as described (20). AMP concentrations varied from 0 to 1 mM. The glucose-1-phosphate assays varied the concentration of glucose-1-phosphate from 16 to 200 mM and were run in the absence of AMP.

**Circular Dichroism.** The circular dichroism spectra of phos. *b* and *a* and I13G *b* and *a* were determined in the Iowa State University Protein Facility using a Jasco J-710 spectropolarimeter (Jasco Corporation, Tokyo, Japan). Samples were diluted in 10 mM phosphate buffer, pH 6.8. Phosphorylase was diluted to 0.1 mg/mL for the analysis. The

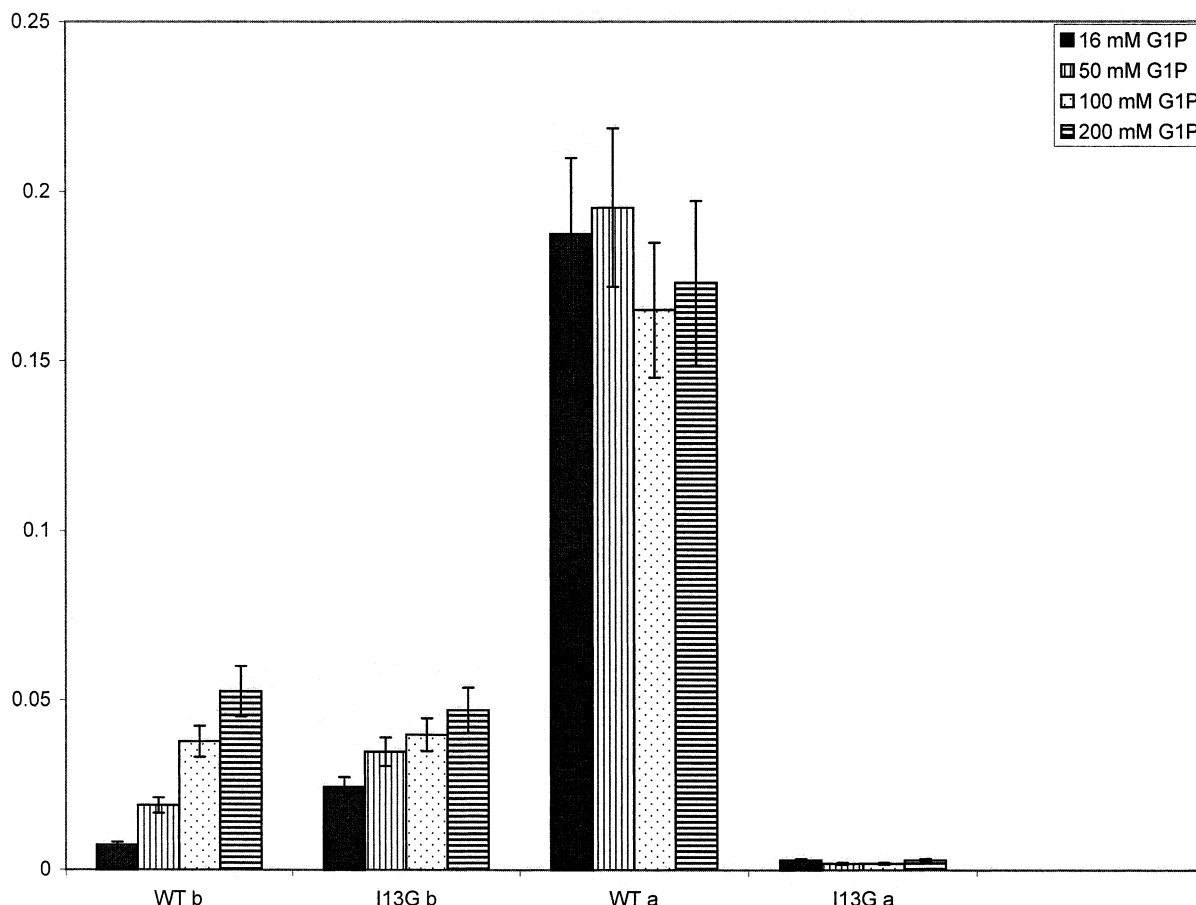


FIGURE 2: Effect of glucose-1-phosphate on wild-type and I13G phosphorylases. Wild-type and I13G phosphorylases *b* and *a* were assayed in the presence of increasing concentrations of glucose-1-phosphate. The concentrations of glucose-1-phosphate utilized for this experiment were 16, 50, 100, and 200 mM. All assays were conducted in the absence of AMP. These analyses were repeated a minimum of three times in triplicate on at least three separate occasions.

wavelength scan was run from 200 to 260 nm utilizing a 0.1 cm cell.

**Analytical Ultracentrifugation.** Equilibrium velocity centrifugation of phos. *b* and *a* and I13G *b* and *a* was performed in the Iowa State University Protein Facility using a model XL-A Maxima Optima Beckman centrifuge. Data were analyzed with Beckman XL-A software. Samples were in 40 mM  $\beta$ -glycerol phosphate, pH 6.8, 100 mM KCl.

**Assays of Protein Phosphatase Activities.** PP-1 assays were performed as previously described (21). The final assay mixture of 0.1 mL contained 0.2 mg/mL [ $^{32}$ P]phos. *a*, 50 mM imidazole, pH 7.2, 2 mM dithiothreitol, 0.5 mg/mL bovine serum albumin, 5 mM caffeine, and 0.2 mM  $\text{MnCl}_2$ . The concentration of PP-1 was 0.5 U/mL. For AP, the 0.1 mL reactions contained 25 mM Tris, pH 8.0, 1 mM  $\text{MgCl}_2$ , 0.2 mg/mL [ $^{32}$ P]phos. *a*, 2 mM dithiothreitol, 0.5 mg/mL bovine serum albumin, and 5 mM caffeine. The concentration of AP was 86.4 U/mL. The reaction conditions used for PP-2A were the same as for PP-1, except the PP-2A concentration was 10 U/mL. Assays with CaN contained 25 mM Mops, pH 7.0, 1 mM  $\text{MnCl}_2$ , 10  $\mu\text{g/mL}$  calmodulin, 0.1 mM  $\text{CaCl}_2$ , 2 mM dithiothreitol, 0.5 mg/mL bovine serum albumin, 5 mM caffeine, 0.2 mg/mL [ $^{32}$ P]phos. *a*, and 10  $\mu\text{g/mL}$  calcineurin. The phosphorylase inhibitor caffeine, which induces an inactive conformation of phosphorylase *a*, was included in all assays as this confers the conformation preferred by PP-1. Reactions were started with the addition of the specified protein phosphatase. Samples were incubated

at 30 °C for 5–20 min. Reactions were terminated by the addition of 10  $\mu\text{L}$  of 100% trichloroacetic acid. Samples were microcentrifuged for 10 min to precipitate protein. A total of 50  $\mu\text{L}$  of supernatant was spotted into 10 mL of scintillation cocktail and counted to determine the pmol  $^{32}\text{P}$  released. Kinetic data were analyzed with Enzyme Kinetics (Trinity Software). Phos. *a* concentrations varied from 0.4 to 20  $\mu\text{M}$  depending on the mutant phos. *a* utilized.

## RESULTS

**Characterization of Phosphorylase *a* Mutants.** Phos. *a* R16A, R16E, I13G, R69K, and R69E activities were assayed in the presence and absence of AMP. After phosphorylation, the activity of phos. *a* in the absence of AMP should be equivalent to the activity in the presence of AMP. As shown in Figure 1, phos. *a*, R16A, R16E, and R69K all exhibited similar activities with and without AMP. Interestingly, I13G had no detectable activity in the absence of AMP. Phosphorylation activated R69E but only to 70% of the level observed with AMP. These data are consistent with what we previously reported (22).

**Structural Characterization of I13G Mutant.** The lack of activity observed in I13G after phosphorylation led us to examine the secondary structure of this mutant as compared to phos. *a*. The N-terminal phosphorylatable region in phos. *b*, residues 10–18, appears to be in a random conformation (11). Upon phosphorylation, the N-terminus of phos. *a* rotates

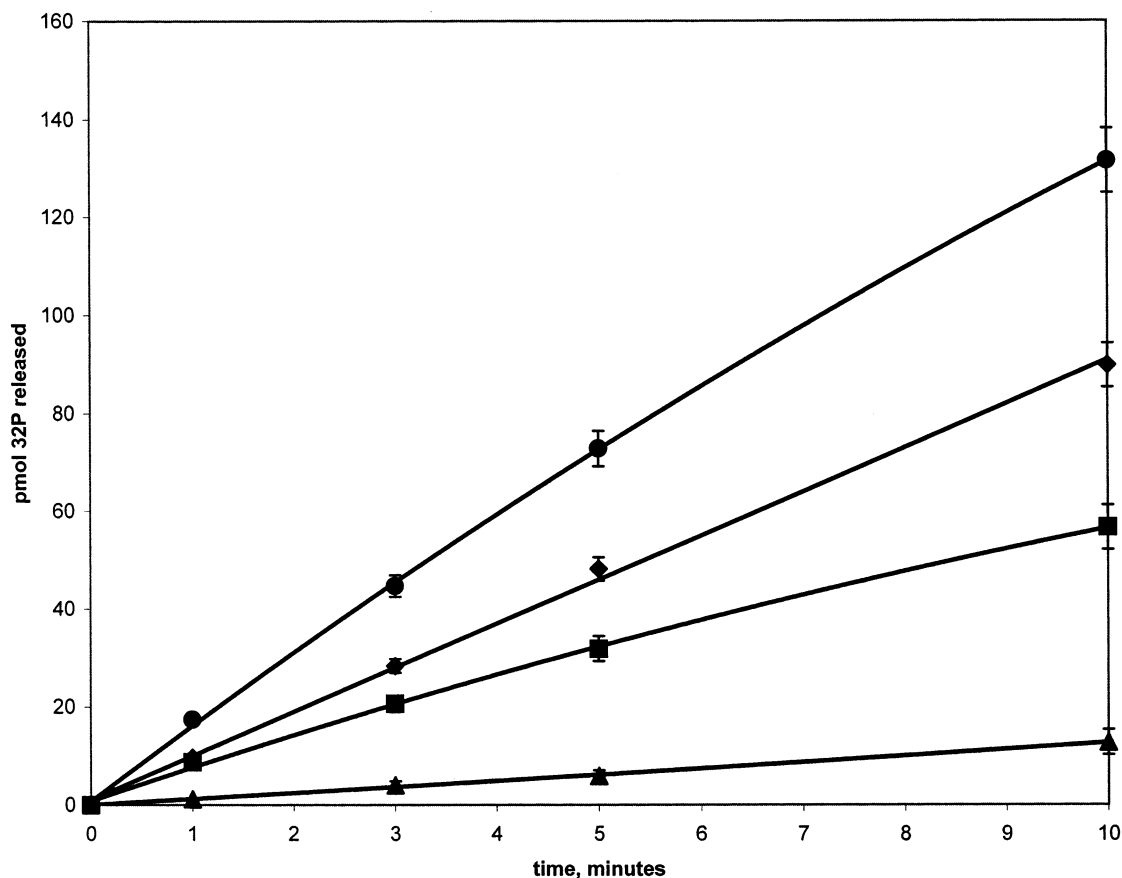


FIGURE 3: Time course of dephosphorylation for N-terminal phosphorylase mutants. Dephosphorylation of (◆) wild-type, (■) R16A, (▲) R16E, and (●) I13G with protein phosphatase-1. Dephosphorylation is reported in picomoles of  $^{32}\text{P}$  released. The assay contained 0.2 mg/mL of the specified [ $^{32}\text{P}$ ] phosphorylase. Reactions were initiated by the addition of 0.5 U/mL of protein phosphatase-1. All analyses were repeated a minimum of three times in triplicate on at least three separate occasions with a minimum of three different protein preparations.

up and interacts at the subunit interface, with a  $3_{10}$  helix forming around the phosphorylated serine (11). We wanted to see if we could detect this change in I13G using CD. CD spectra were collected and compared for phosphorylase and I13G in the *b* and *a* forms. The secondary structures of phos. *b* and I13G are almost identical (data not shown). The secondary structures of the phosphorylated phos. *a* and I13G are again very similar, indicating that a change in secondary structure has occurred in I13G upon phosphorylation (data not shown). However, this change did not result in activation of phosphorylase. The quaternary structures of phos. *b* and *a* were also compared to I13G *b* and *a* using equilibrium velocity centrifugation. Phos. *b* exists as a dimer of 195 kDa, and phos. *a* forms a tetramer of 390 kDa. The calculated molecular weight for I13G was 215 kDa, and phosphorylated I13G was 197 kDa (data not shown). Thus, it appeared that I13G remained a dimer after phosphorylation.

**Functional Characterization of I13G Mutant.** Phos. *b* can be activated allosterically by AMP and is inactive without it. Phos. *b* cooperatively binds AMP, while phos. *a* does not (23). I13G has no activity after phosphorylation, and the AMP binding of I13G appears to be more like phos. *b* (22). Thus, it is possible that phosphorylated I13G might be similar to phos. *b*. The classic model of cooperativity is based on the existence of multiple conformational states, ranging from a T state, with low affinity for substrate, to an R state, with high affinity for substrate. Phos. *b* (T state) has a  $K_m$  of 50 mM for its substrate glucose-1-phosphate, whereas phos. *a* (R state) has a  $K_m$  of 3.8 mM (24). As shown in Figure 2,

both phos. *b* and I13G exhibited increased activities with increased glucose-1-phosphate in the absence of AMP. No activity was detected, however, in any of the phosphorylated I13G samples. From these data, phosphorylated I13G appears to be more like T state than R state.

**Dephosphorylation of Mutant Phosphorylase *a* by Select Phosphatases.** Dephosphorylation of phos. *a* was compared to dephosphorylation of the N-terminal mutants R16A, R16E, and I13G using PP-1. Figure 3 illustrates the time course of dephosphorylation. PP-1 dephosphorylated all of the phos. *a*'s to varying extents. R16E was dephosphorylated at the lowest rate. R16A was dephosphorylated at a rate approximately one-half that of phos. *a*, while I13G was dephosphorylated at a faster initial rate. Figure 4 demonstrates the time course of PP-1 dephosphorylation of phos. *a* as compared to the two R69 mutations, R69K and R69E. The R69 mutants were dephosphorylated similarly to phos. *a*. However, the R69 mutations seem to be slightly preferred substrates for PP-1.

Figure 5 illustrates the differences in dephosphorylation of phos. *a* as compared to the N-terminal mutants, R16A, R16E, and I13G, with PP-1, PP-2A, AP, and CaN. Dephosphorylation is reported as percent activity as compared to PP-1 dephosphorylation of phos. *a*, which is set at 100%. Consistent with the time course of dephosphorylation presented in Figure 3, PP-1 dephosphorylated all of the phos. *a*'s to different extents. R16E was the least preferred substrate for PP-1. R16A was dephosphorylated at a rate about 50% of phos. *a*, and I13G was actually a better substrate than



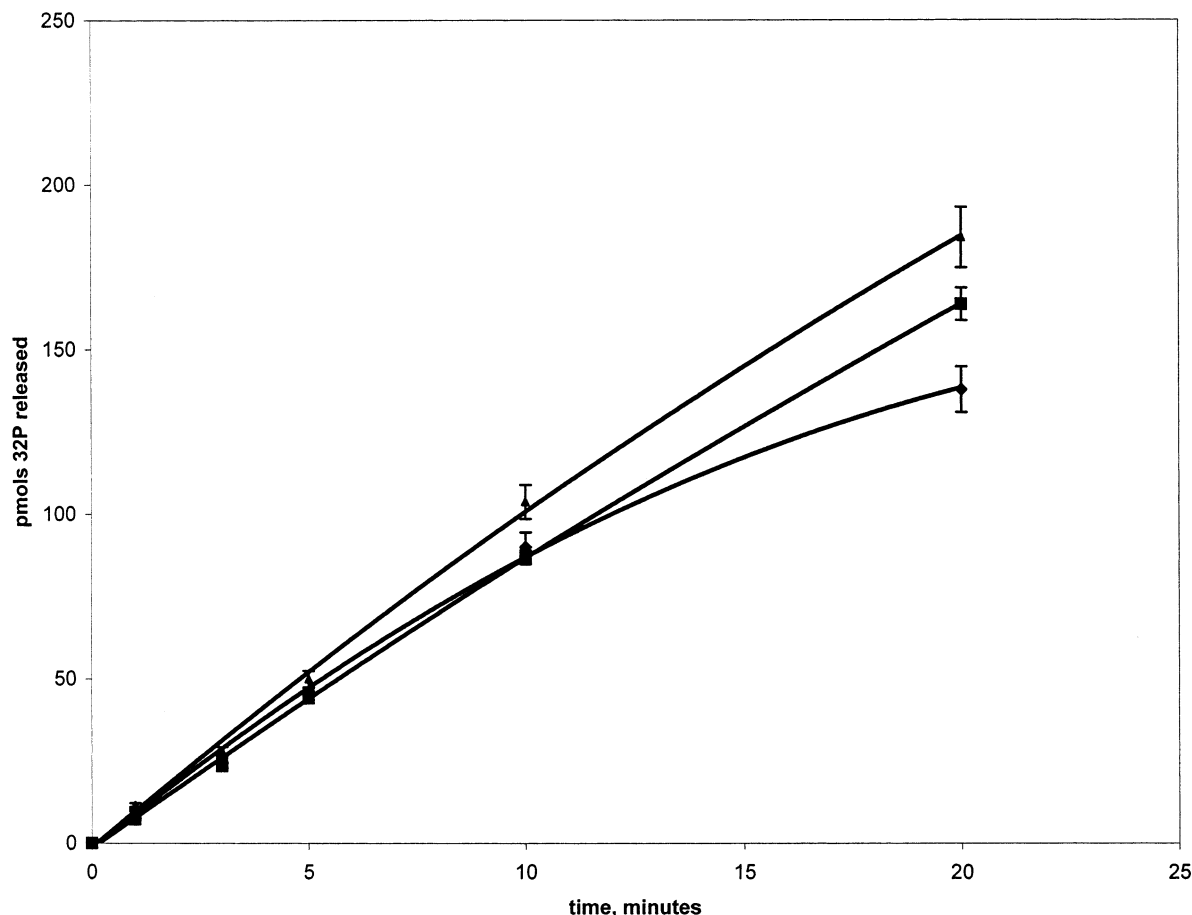


FIGURE 4: Time course of dephosphorylation for the phosphoserine interaction mutants. Dephosphorylation of (◆) wild-type, (■) R69K, and (▲) R69E with protein phosphatase-1 reported in picomoles of  $^{32}\text{P}$  released. The assay contained 0.2 mg/mL of the specified [ $^{32}\text{P}$ ] phosphorylase. Reactions were initiated by the addition of 0.5 U/mL of protein phosphatase-1. All analyses were repeated a minimum of three times in triplicate on at least three separate occasions with a minimum of three different protein preparations.

phos. *a*. PP-2A dephosphorylated phos. *a* and R16A equally and preferred R16E the least. I13G was again preferred, as compared to phos. *a*, 63 versus 21%. CaN followed the same substrate preference pattern of PP-2A, albeit to a lesser extent for I13G. No significant dephosphorylation of phos. *a* or any mutant was detected using AP.

Comparison of the mutants R69K and R69E to phos. *a* using different phosphatases can also be seen in Figure 5. Consistent with the time course of dephosphorylation (Figure 4), the R69 mutants were preferentially dephosphorylated by PP-1, with R69E favored over R69K. This pattern was repeated by PP-2A. CaN preferred the R69 mutants over phos. *a* and did not appear to distinguish between R69K and R69E. No significant dephosphorylation of phos. *a* or any mutant was detected using AP. In Figure 5, higher concentrations of the other protein phosphatases (PP-2A, CaN, and AP) were used than of PP-1 (see Experimental Procedures for concentrations utilized of each phosphatase).

**Kinetic Analyses of Dephosphorylation by PP-1.** Table 1 summarizes the kinetic parameters for dephosphorylation of phos. *a* as compared with R16A, R16E, I13G, R69K, and R69E using PP-1. All experiments were run using equivalent phosphate to calculate the concentration of mutants that were not 100% phosphorylated. The  $K_m$  for I13G was similar to the  $K_m$  for phos. *a*, although the  $V_{max}$  was 2-fold greater for I13G than that for phos. *a*. R16E exhibited approximately a 3-fold increase in  $K_m$  and a 6.5-fold decrease in  $V_{max}$ . R16A

had a similar  $K_m$  to phos. *a* but had a 3.3-fold lower  $V_{max}$ . As seen with I13G, the  $K_m$  for R69K was similar to phos. *a*, and the  $V_{max}$  was approximately 3-fold greater. The most drastic changes observed occurred with the R69E mutant. This mutant exhibited a 4-fold higher  $K_m$  and a 10.5-fold increase in  $V_{max}$ , as compared to phos. *a*.

## DISCUSSION

In this work, we were interested in addressing the structural basis for recognition of phos. *a* by specific phosphatases, PP-1 in particular. What makes the dephosphorylation reaction much more effective with protein substrate as compared to phosphopeptide substrate? Why do some phosphatases, AP for example, dephosphorylate phospho-9–18 peptide but do not dephosphorylate phos. *a*? Mutants of phos. *a* were made to address this question of specificity.

Prior to utilizing the phosphorylase mutants as protein substrates for PP-1, it was important to examine the activity of the phosphorylase mutants as an indirect measure of structural integrity. The phos. *a* mutants R16A and R16E were active in the presence of AMP, as well as in the absence of AMP after phosphorylation. Both mutants exhibited activities very similar to phos. *a*. Both of the R69 mutations were active. These results indicated that these phosphorylase mutants appear to be viable PP-1 protein substrates (Figure 1). Although I13G shows activity similar to phos. *a* in the presence of AMP, we were unable to detect any phos. *a*

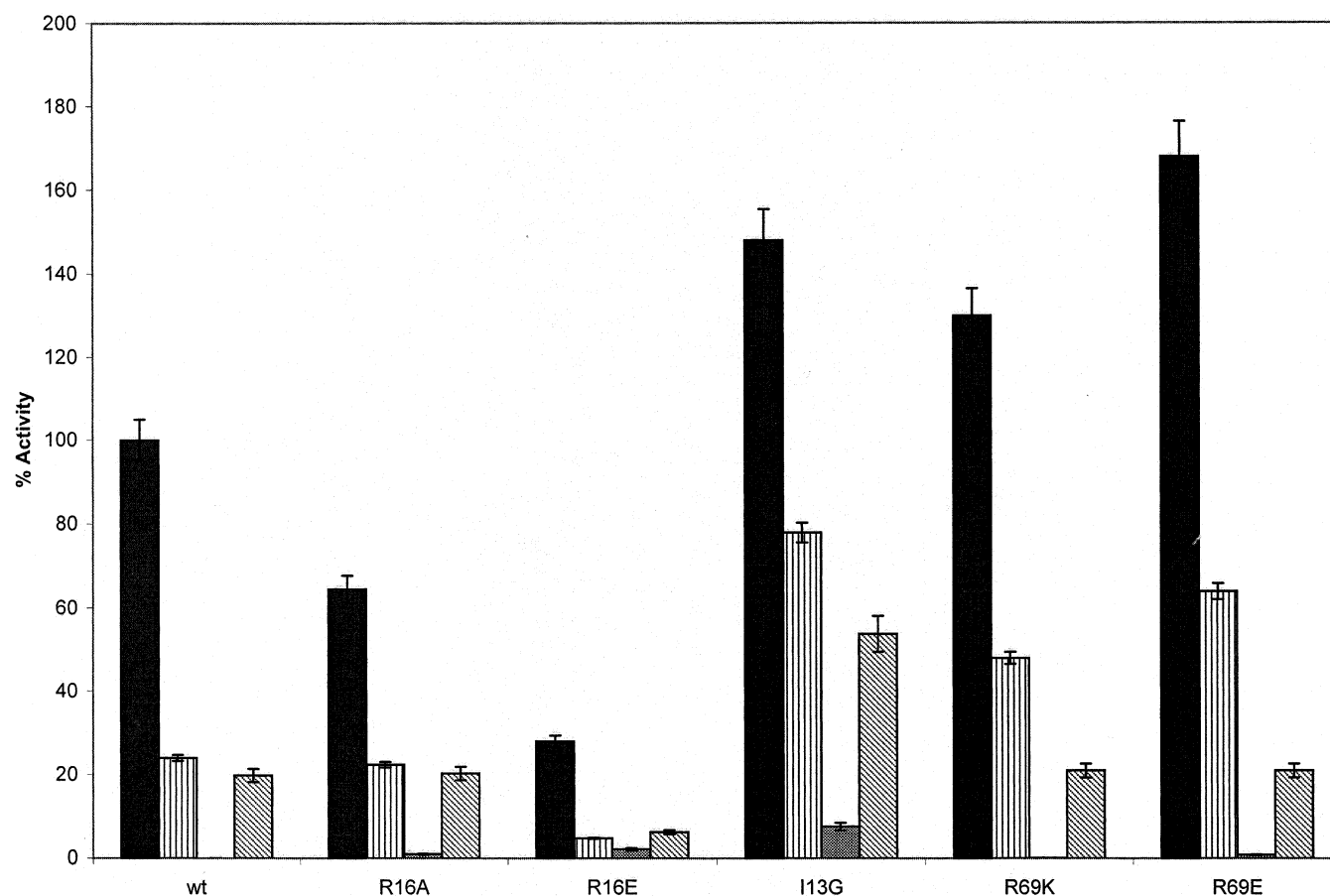


FIGURE 5: Dephosphorylation of the phosphorylase mutants by different protein phosphatases. Dephosphorylation is reported as % dephosphorylation as compared to wild type with protein phosphatase dephosphorylation of phosphorylase set at 100%. All reactions were initiated with the addition of the specified phosphatases. Units utilized were as follows: 0.5 U/mL protein phosphatase-1, 10 U/mL protein phosphatase-2A, 86.4 U/mL alkaline phosphatase, and 10  $\mu$ g/mL calcineurin. The concentrations of phosphorylases were 0.2 mg/mL. Reactions were run for 20 min. These analyses were repeated a minimum of three times in triplicate on at least three separate occasions.

Table 1: Kinetic Constants for Phosphorylase Mutants with Protein Phosphatase-1

	$K_m$ ( $\mu$ M)	$V_{max}$ (nmol P/min/mg)
wild type	$0.94 \pm 0.05$	$5124 \pm 600$
R16A	$1.46 \pm 0.3$	$1533 \pm 200$
R16E	$3.4 \pm 0.3$	$778 \pm 150$
I13G	$1.0 \pm 0.14$	$13\,208 \pm 1500$
R69K	$1.12 \pm 0.3$	$14\,429 \pm 2500$
R69E	$4.33 \pm 0.5$	$54\,315 \pm 10\,000$

activity in the absence of AMP after phosphorylation. Because its AMP-induced activity was intact, however, we determined that I13G was also a viable mutant.

The lack of I13Ga activity prompted its further characterization as compared to *phos. b* and *phos. a*. In the crystal structure of *phos. b*, the N-terminus, containing the phosphorylatable serine, forms a random structure. After phosphorylation, the structure of the N-terminus changes to a  $3_{10}$  helix and rotates up to the subunit interface, initiating a conformational change to the activated state. Although we cannot detect such conformational changes directly, the absence of activity in phosphorylated I13G suggests that its conformation has not changed to the activated state. The CD spectra indicate that the overall secondary structures of I13Gb and I13Ga do not differ significantly from *phos. b* and *a*. The conformational change occurring upon phosphorylation of I13G, however, is not the same change that occurs in *phos.*

*a*. (Figures 1 and 2). The results from equilibrium velocity centrifugation indicate that phosphorylated I13G is a dimer. These data further confirm the same conclusions we reported previously (22). It is likely that the Gly in place of the Ile disrupts the  $3_{10}$  helix, not allowing proper positioning of the seryl phosphate, which appears necessary for activation and tetramer formation.

In addition, while *phos. b*, *phos. a*, and I13Gb are active in the absence of AMP with increasing G1P concentration, I13Ga is not (Figure 2). These results are still consistent with I13Ga being similar to the T state. This T state of I13Ga, however, cannot function exactly like *phos. b* because of the phosphate group on the N-terminus. The unphosphorylated N-terminus plays an important role in *phos. b* effector and substrate binding (22). Therefore, it follows that I13Ga will not have all of the same characteristics as *phos. b*, exemplified by its lack of activation by G1P.

Once the N-terminus has moved to the subunit interface after phosphorylation, many interactions stabilize it in that position in *phos. a* (11). NMR studies show an interaction of Arg 16 with the phosphoserine in peptide substrate (6). The crystal structure of *phos. a* shows the phosphoserine complexed with Arg 69 and Arg43', from the opposite subunit (11). All of these interactions may be part of the recognition motif for PP-1 and contribute to its overall specificity for glycogen phosphorylase.

Substitution of Arg 16 with citrulline in peptide substrate derivatives of 9–18, a peptide of the phosphorylated region of phos. *a*, resulted in decreased dephosphorylation of this peptide by PP-1 (6). Our results confirm the importance of Arg 16 for phos. *a* recognition by PP-1. Both of the Arg 16 phos. *a* mutants, R16A and R16E, were dephosphorylated by PP-1 at a lesser rate. The  $K_m$  and  $V_{max}$  for R16E change significantly. R16A has a similar  $K_m$  as compared to phos. *a*, but the  $V_{max}$  decreases. It appears that PP-1 does prefer the positive charge of Arg 16 for optimal turnover, but it will dephosphorylate the R16A and R16E mutants. It was suggested in the peptide studies that Arg 16 either enhances substrate turnover for PP-1, or alternatively, that PP-1 recognizes the complex formed from the interaction of an Arg with the target phosphoserine (6). This interaction could be with Arg16 or with residues Arg 69 and Arg 43' in phos. *a*.

Our results with R69K and R69E indicate that this residue is also important for PP-1 recognition but for different reasons. Both Arg 69 mutants are dephosphorylated preferentially to phos. *a* by PP-1 and 2A. Although R69K has an increased  $V_{max}$ , the  $K_m$  is the same as phos. *a*. R69E *a* has a drastically increased  $V_{max}$  but also an increased  $K_m$ . Nevertheless, it is also a slightly better substrate for PP-1. The charge reversal at this position could result in the seryl phosphate being electrostatically repelled and not able to make its usual contacts. This could lead to the seryl phosphate being more exposed and accessible to the phosphatase. So, while Arg 16 seems to be a positive determinant for PP-1 recognition, Arg 69 may be a negative determinant, keeping the phosphate initially hidden. From these results, it is difficult to say whether PP-1 uses Arg 69 as a specificity determinant. For I13G, the similarity in the  $K_m$  as compared to phos. *a* indicates that PP-1 recognizes similar features common to both of these conformations of phos. *a*. The increased  $V_{max}$  for I13G indicates that it is also a better substrate than phos. *a* and may be due to a more accessible phosphoserine residue. Our thorough characterization of I13G does indicate a disrupted N-terminal structure, which may expose the phosphate as in R69E, perhaps to an even greater extent than R69E. Increased accessibility of the phosphoserine residue might also explain why I13G was dephosphorylated to a greater extent by PP-2A and CaN.

Therefore, it seems that the specificity of PP-1 for phos. *a* does not reside with just a few residues. With the exception of Arg 16, which does seem to be a positively recognized residue, the other residue changes actually produced better substrates for PP-1. These increases in dephosphorylation seem, however, to be due mostly to phosphate accessibility. It is most likely, then, that the overall phos. *a* conformation is what is primarily recognized by PP-1. This also explains why peptides are poorer substrates for phosphatases. AP was able to dephosphorylate the citrulline-substituted phospho-

peptides of phos. *a*, yet we were unable to detect any significant dephosphorylation of phos. *a* or any of the mutants with AP. These results again emphasize protein phosphatase specificity for higher order structure in addition to the primary structure. Further work involving mutagenesis of phos. *a*, as well as other physiologically relevant protein phosphatase substrates is warranted. If mutants could be found that drastically changed the phos. *a* conformation without changing the N-terminal structure, these might provide more specific answers to what is conformationally recognized. The combination of available crystal structures of phos. *a* with the crystal structure of PP-1 should also help guide the planning of future experiments. Additional experiments with phosphoprotein substrates of protein phosphatases will help broaden our understanding of protein phosphatase substrate specificity.

## REFERENCES

1. Ingebritsen, T. S., and Cohen, P. (1983) *Science* 221, 331–338.
2. Bollen, M., and Stalmans, W. (1992) *Crit. Rev. Biochem. Molec. Biol.* 27, 227–281.
3. Pinna, L. A., and Donella-Deana, A. (1994) *Biochim. Biophys. Acta* 1222, 415–431.
4. Graves, D. J., Fischer, E. H., and Krebs, E. G. (1960) *JBC* 235, 805–809.
5. Graves, D. J., Martensen, T. M., Tu, J.-I., and Tessmer, G. M. (1973) in *Third International Symposium held in Seattle June 5–8*, pp 53–61, Springer-Verlag.
6. Martin, B. L., Luo, S., Kintanar, A., Chen, M., and Graves, D. J. (1998) *Arch. Biochem. Biophys.* 359, 179–191.
7. Zhang, L., and Lee, E. Y. C. (1997) *Biochemistry* 36, 8209–8214.
8. Kemp, B., Graves, D., Benjamini, E., and Krebs, E. (1977) *J. Biol. Chem.* 252, 4888–4894.
9. Biorn, A., Bartleson, C., and Graves, D. (2000) *Biochemistry* 39, 15887–15894.
10. Chou, P., and Fasman, G. (1978) *Adv. Enzymol.* 47, 45–148.
11. Barford, D., Hu, S.-H., and Johnson, L. N. (1991) *J. Molec. Biol.* 218, 233–260.
12. Huang, C.-Y. F., Yuan, C.-J., Livanova, N. B., and Graves, D. J. (1993) *Molec. Cell. Biochem.* 127/128, 7–18.
13. Krebs, E. G., Kent, A. B., Graves, D. J., and Fischer, E. H. (1958) *Proc. Intl. Symp. Enzyme Chem.* 1957 1, 41–43.
14. Browner, M. F., Rasor, P., Tugendreich, S., and Fletterick, R. J. (1991) *Protein Eng.* 4, 351–357.
15. Luong, C. B. H., Browner, M. F., and Fletterick, R. J. (1992) *J. Chromatogr.* 584, 77–84.
16. Kastenschmidt, L. L., Kastenschmidt, J., and Helmreich, E. (1968) *Biochemistry* 17, 3590–3608.
17. Krebs, E. G., and Fischer, E. H. (1962) *Methods Enzymol.* 5, 373–376.
18. Reimann, E. M., Walsh, D., and Krebs, E. G. (1971) *JBC* 246, 1986–1995.
19. Illingworth, B., and Cori, C. F. (1953) *Biochem. Prepr.* 3, 1–9.
20. Krebs, E. G., Love, D. S., Bratvold, G. E., Trayser, K. A., and Fischer, E. H. (1964) *Biochemistry* 3, 1022–1033.
21. Killilea, S. D., Aylward, J. H., Mellgren, R. L., and Lee, E. Y. C. (1978) *Arch. Biochem. Biophys.* 191, 638–646.
22. Biorn, A., and Graves, D. (2001) *Biochemistry* 40, 5181–5189.
23. Johnson, L. N., and Barford, D. (1990) *JBC* 265, 2409–2412.
24. Uhing, R. J., Lentz, S. R., and Graves, D. J. (1981) *Biochemistry* 20, 2537–2544.

BI027091S